



Centrum voor Wiskunde en Informatica

**REPORT***RAPPORT*

Multigrid methods for high-order accurate fully implicit simulation  
of flow in porous media

J. Molenaar

Department of Analysis, Algebra and Geometry

**AM-R9605 May 31, 1996**

Report AM-R9605  
ISSN 0924-2953

CWI  
P.O. Box 94079  
1090 GB Amsterdam  
The Netherlands

CWI is the National Research Institute for Mathematics and Computer Science. CWI is part of the Stichting Mathematisch Centrum (SMC), the Dutch foundation for promotion of mathematics and computer science and their applications.

SMC is sponsored by the Netherlands Organization for Scientific Research (NWO). CWI is a member of ERCIM, the European Research Consortium for Informatics and Mathematics.

Copyright © Stichting Mathematisch Centrum  
P.O. Box 94079, 1090 GB Amsterdam (NL)  
Kruislaan 413, 1098 SJ Amsterdam (NL)  
Telephone +31 20 592 9333  
Telefax +31 20 592 4199

# Multigrid Methods for High-Order Accurate Fully Implicit Simulation of Flow in Porous Media \*

J. Molenaar

CWI

*P.O. Box 94079, 1090 GB Amsterdam, The Netherlands*

## Abstract

High-order accurate finite difference schemes are widely used to avoid the detrimental effects of numerical diffusion in first-order upwind schemes. If an implicit time integration scheme is employed, we have to solve large systems of nonlinear equations in every time step. The price paid for the high-order accuracy is a larger discretization stencil. In this paper we consider the use of multigrid methods for the iterative solutions of these systems of equations. We consider both a direct multigrid approach and a defect correction approach, in which only first-order accurate discretized problems have to be solved. In both approaches we do not need to store the Jacobean matrix. Therefore the memory requirements are moderate, and very fine grid simulations are feasible on a standard workstation.

*AMS Subject Classification (1991):* 65M06, 65M55, 76S05, 76T05

*Keywords & Phrases:* multigrid, second-order accurate discretizations, defect correction

## 1. INTRODUCTION

In many important areas of porous media flow simulation, like petrol reservoir engineering, environmental studies, etc., one has to deal with convection dominated flows. To obtain a good resolution of moving fronts it is attractive in finite difference methods to use a second-order accurate space discretization. For stability reasons it is desirable to use an implicit time integration method. This means that large systems of nonlinear equations have to be solved in every time step. In this paper we study the possibility of using multigrid methods for this task.

We consider two possibilities. A straightforward approach is to apply multigrid directly to the second-order discretized equations. The other possibility is to use a defect correction iteration with a first-order space discretization. The first-order equations are then solved approximately by a multigrid method.

In this paper we focus on immiscible and miscible flow problems that are characterized by adverse displacement ratios. These problems are infamous for the so-called grid orientation effects. That means that the numerical solution depends strongly on the orientation and size of the grid. There exist an enormous literature on this subject (see e.g., [1],[2],[5]). Without any diffusive term these problems are physically unstable. Only if the physical

---

\*To appear in "Proceedings ECCOMAS 96".

diffusion dominates the numerical diffusion, the grid orientation effects are expected to vanish. Therefore these problems are good test problems for our purposes. They necessitate the use of fine discretization grids, and thus make it possible to study the efficiency of multigrid methods in general, and to compare the direct multigrid approach to the defect correction method.

## 2. MODEL EQUATIONS

The model equations describing miscible and two-phase immiscible flow are quite similar. Neglecting capillary effects and gravity the model equations for incompressible and immiscible two-phase flow in a homogeneous medium are

$$-\nabla \cdot \lambda_t(s) \nabla p = \nabla \cdot \mathbf{q}_t = Q_t, \quad (2.1)$$

$$\frac{\partial s}{\partial t} + \nabla \cdot f_w(s) \mathbf{q}_t = Q_w, \quad (2.2)$$

where the subscripts  $w$  and  $o$  refer to the water and oil,  $\lambda_t = \lambda_w + \lambda_o$ ,  $\lambda_\alpha$  is the phase mobility,

$$\lambda_\alpha = \frac{k_\alpha(s)}{\mu_\alpha}, \quad (2.3)$$

$k_\alpha$  the phase relative permeability,  $\mu_\alpha$  the phase viscosity,  $f_w = \lambda_w/\lambda_t$  the fractional flow function, and  $Q_w$ ,  $Q_t$  the injection/production rates. In the model equations (2.1)–(2.2) the pressure  $p$  and the water saturation  $s$  are the primary unknowns. The fractional flow function  $f_w$  determines the shape and height of any occurring shocks. The frontal mobility ratio  $M$  is the ratio of the phase mobilities upstream and downstream of a shock. For  $M > 1$  the problem is physically unstable.

For fully miscible displacement the model equations are

$$-\nabla \cdot \frac{1}{\mu(c)} \nabla p = \nabla \cdot \mathbf{q}_t = Q_t, \quad (2.4)$$

$$\frac{\partial c}{\partial t} + \nabla \cdot (c \mathbf{q}_t - D \nabla c) = Q_c, \quad (2.5)$$

where  $c$  denotes the concentration of the injected fluid. The viscosity of the mixture is given by

$$\mu(c) = \left(1 - c + M^{\frac{1}{4}} c\right)^{-4}. \quad (2.6)$$

The physical dispersion tensor  $D$  represents a velocity dependent diffusion of magnitude  $D_l |\mathbf{q}_t|$  in the flow direction, a velocity dependent diffusion of magnitude  $D_t |\mathbf{q}_t|$  in the direction transversal to the flow and a molecular diffusion term  $D_m$ .

## 3. DISCRETIZATION

Let us first consider the discretization of the immiscible two-phase flow equations (2.1)–(2.2). A standard approach for the numerical solution of these equations consists of a cell-centered

finite difference discretization in space, combined with a backward Euler time integration. In one space dimension this leads to a discretization for the pressure equation (2.1) of the form

$$\lambda_{t_{i-1/2}}^{n+1} \frac{p_i^{n+1} - p_{i-1}^{n+1}}{\Delta x} - \lambda_{t_{i+1/2}}^{n+1} \frac{p_{i+1}^{n+1} - p_i^{n+1}}{\Delta x} = \Delta x Q_{t_i}^{n+1}. \quad (3.7)$$

We approximate  $\lambda_{t_{i+1/2}}$  by a harmonic average,

$$\lambda_{t_{i+1/2}} = \frac{2\lambda_{t_i}\lambda_{t_{i+1}}}{\lambda_{t_i} + \lambda_{t_{i+1}}}. \quad (3.8)$$

The transport equation (2.2) is discretized by

$$\frac{s_i^{n+1} - s_i^n}{\Delta t} + \frac{f_{w_{i+1/2}}^{n+1} - f_{w_{i-1/2}}^{n+1}}{\Delta x} = Q_{t_i}^{n+1}. \quad (3.9)$$

Usually some form of upstream weighting is used to define the numerical flux  $f_{w_{i+1/2}}$ . The use of one-point upstream weighting leads to a scheme that is formally first-order consistent in space. This scheme suffers from strong numerical diffusion, i.e., sharp fronts are smeared out. Moreover the numerical diffusion term is anisotropic, so there are strong grid orientation effects. The use of simple second-order accurate weighting schemes, like the two-point upstream scheme (see [8]), causes spurious oscillations near sharp fronts in the solution. Therefore a limited interpolation is used for the saturations  $s$  to obtain a left approximation  $s_{i+1/2}^l$  and a right approximation  $s_{i+1/2}^r$ ,

$$s_{i+1/2}^l = s_i + \frac{1}{2}\psi(r_{i+1/2}^l)(s_i - s_{i-1}), \quad (3.10)$$

$$s_{i+1/2}^r = s_{i+1} + \frac{1}{2}\psi(r_{i+1/2}^r)(s_{i+2} - s_{i+1}), \quad (3.11)$$

where  $r$  denotes the ratio of consecutive gradients,

$$r_{i+1/2}^l = \frac{s_{i+1} - s_i}{s_i - s_{i-1}}, \quad (3.12)$$

$$r_{i+1/2}^r = \frac{s_{i+1} - s_i}{s_{i+2} - s_{i+1}}, \quad (3.13)$$

and  $\psi(r)$  the so-called limiter function. Here we use the limiter proposed by Van Leer [6],

$$\psi(r) = \frac{r + |r|}{1 + |r|}. \quad (3.14)$$

The numerical flux  $f_{w_{i+1/2}}^{n+1}$  is the Godunov flux, i.e., the flux corresponding the state  $s_{i+1/2}$  that propagates with zero speed in the Riemann problem with initial left and right values  $s_{i+1/2}^l$  and  $s_{i+1/2}^r$ . We remark that by taking  $\psi \equiv 0$  we retain the standard first-order upwind scheme.

The backward Euler scheme is formally only first-order accurate in time. However, a second-order accurate scheme in both space and time is obtained by replacing the backward Euler scheme by the Crank-Nicholson scheme.

The discretization of the miscible flow problem is nearly identical to that of the two-phase immiscible flow problem. The only difference is the extra dispersion/diffusion term. For the discretization of this second order term we use a standard nine-point scheme.

#### 4. MULTIGRID AND DEFECT CORRECTION

The implicit time integration necessitates the solution of large systems of nonlinear equations in every time step. We consider the possibility of applying multigrid methods for the iterative solution of these systems of equations. Good multigrid convergence rates have been observed for the one-point upstream discretization of the two-phase flow equations (see [3],[7]).

As yet it is not clear whether multigrid can be used for solving the equations obtained by the more accurate discretization, where a limited interpolation for the interface values is used. Let  $\mathcal{N}_h^1(u)$  denote the standard first-order upwind discretization ( $\psi \equiv 0$ ), and  $\mathcal{N}_h^2(u)$  the second-order accurate scheme. We now consider two ways of applying multigrid.

The first approach is a direct nonlinear multigrid approach. We consider a cell-centered multigrid method. In cell-centered multigrid methods the coarser grids  $G_{2h}$ ,  $G_{4h}$ ,  $\dots$  are constructed by successively doubling the mesh width of the fine grid  $G_h$ . Hence, each coarse grid cell is the union of four fine grid cells. Suppose that on the fine grid  $G_h$  we have the system of equations

$$\mathcal{N}_h^2(u_h) = 0. \quad (4.15)$$

The coarse grid corrections that we consider are of the form

$$\mathcal{N}_{2h}^2(u_{2h}^{(i+1)}) = \mathcal{N}_{2h}^2(u_{2h}^{(i)}) - \overline{R}_{2h}^h \mathcal{N}_h^2(u_h^{(i)}), \quad (4.16)$$

$$u_h^{(i+1)} = u_h^{(i)} + \tilde{P}_h^{2h} \left( u_{2h}^{(i+1)} - u_{2h}^{(i)} \right), \quad (4.17)$$

where  $\overline{R}_{2h}^h$  denotes the restriction that is the adjoint of the interpolation by a piecewise constant function. In the cell centered multigrid method this is natural: the residual (the total excess of accumulation and net flow) in a coarse grid cell is the sum of the residuals in the corresponding four fine grid cells. The prolongation  $\tilde{P}_h^{2h}$  is the piecewise bilinear interpolation. This combination of prolongation and restriction is formally sufficiently accurate to deal with second-order partial differential equations. We obtain the coarse grid operator  $\mathcal{N}_{2h}^2(u_{2h})$  by discretization on the coarse grid (i.e., a grid with mesh size  $2h$ ). For  $u_{2h}^{(i)}$  we take

$$u_{2h}^{(i)} = R_{2h}^h u_h^{(i)}, \quad (4.18)$$

where  $R_{2h}^h$  is the adjoint of interpolation by piecewise constants.

A collective point Gauss-Seidel-Newton relaxation is used as the smoother on all grids in the multigrid algorithm. This means that all cells are visited in some predetermined order, and that the equations (3.7) and (3.9) are solved simultaneously for the variables related

to that cell. This small system of two nonlinear equations is solved by Newton-Raphson iteration. On the coarsest grid in the calculation we use a direct Newton-Raphson solver. This completes our description of the direct multigrid approach.

The second possibility for using multigrid that we consider is a iterative defect correction approach (see [4]). The defect correction iteration is defined by

$$\mathcal{N}_h^1(u_h^{(i+1)}) = \mathcal{N}_h^1(u_h^{(i)}) - \mathcal{N}_h^2(u_h^{(i)}). \quad (4.19)$$

Clearly a fixed point of this iteration is a solution to the second-order discretized equations (4.15). In each defect correction step (4.19) we have to solve a first-order discretized problem. This problem is solved approximately by the nonlinear multigrid method that is described above.

We remark that in both approaches there is no need to calculate or store the full Jacobean matrix. Only local linearizations are used in the relaxation procedure. A consequence is that a relatively small amount of computer memory is needed for the calculations, and very fine grid simulations can be performed on a standard workstation.

## 5. NUMERICAL RESULTS

We now compare the defect correction and the direct multigrid approach for two test problems: a two-phase immiscible and a miscible flow problem. In both cases we consider a repeated five-spot pattern. Two different computational grids are possible that are commonly referred to as the diagonal and the parallel grid (see [5]). We only consider the diagonal grid, in which the primary flow path, from the injection point to the production point, is at an angle of 45 degrees with the grid lines. For this diagonal grid we expect the strongest grid orientation effects.

In all cases we use the second-order accurate Crank-Nicholson scheme for time integration. The time step is chosen adaptively in order to have approximately the same changes in saturation or concentration in every time step. In fact for the immiscible flow problem we take

$$\Delta t^{n+1} = \frac{\Delta s}{\|s^n - s^{n-1}\|_\infty} \Delta t^n. \quad (5.20)$$

The ratio  $\Delta t^{n+1}/\Delta t^n$  is bounded between 0.5 and 2.0, and in our calculations we take  $\Delta s = \Delta c = 0.05$ . The system of discretized equations is solved in every time step with an accuracy of  $10^{-3}$ . This means that in every time step we reduce the  $\ell_1$ -norm of the residual by a factor of  $10^{-3}$ . This is done by a number of multigrid or defect correction sweeps. In the multigrid approach we use F-cycles with one symmetric Gauss-Seidel-Newton sweep for both pre- and post-relaxation. That means that all four possible relaxation directions are being used.

In the defect correction approach we use a single multigrid sweep to solve approximately the first-order accurately discretized equations. The use of more multigrid sweeps hardly improves the convergence behavior. The average convergence rate  $\rho$  for the multigrid method and the defect correction method are defined by

Table 5.1: Statistics for simulation of immiscible flooding.

Grid	$N$	MLTG		DEFCOR	
		$\rho$	$T$	$\rho$	$T$
$20 \times 20$	228	0.09	258	0.04	336
$40 \times 40$	468	0.07	2747	0.04	4261
$80 \times 80$	959	0.06	27181	0.04	52833
$160 \times 160$	1920	0.05	84005	0.04	85261

$\rho$  average convergence rate,  $T$  total run time

$$\rho = \frac{1}{N} \sum_{n=1, N} \left( \frac{\|r^{(m_n)}\|_1}{\|r^{(0_n)}\|_1} \right)^{\frac{1}{m_n}},$$

where  $N$  denotes the total number of time steps, and  $r^{(m_n)}$  the residual after  $m_n$  cycles in time step  $n$ .

### 5.1 Immiscible displacement

We first consider the simulation of the immiscible displacement problem. For this problem we choose  $k_w = s^2$  and  $k_o = (1 - s)^2$  and  $\mu_o/\mu_w = 4$  (see e.g., [2]). This displacement process is in fact stable because the frontal mobility ratio is  $M \approx 0.8$ . Note that we may therefore neglect capillary pressure terms. In Figure 5.1 contour plots are shown of the numerical solution on different grids after 0.45 Pore Volume Injected. The contour lines are drawn at equal intervals of 0.1. The solution consists of a shock followed by a smooth expansion wave from the shock, with theoretical shock height  $s = 0.45$ , towards the injection well where  $s = 1$ . This behavior is clearly shown by the numerical solution in Figure 5.1. There is an excellent representation of the shock on the finest grid used, a  $160 \times 160$  grid, and there are no grid orientation effects. Some simulation statistics for these computations are shown in Table 5.1. Both approaches show a fast grid independent convergence behavior. The defect correction approach converges faster than the direct multigrid approach. Table 5.1 also shows the total execution time  $T$  needed on a SGI-workstation with a 200 MHz CPU. Although the defect correction approach converges faster, and the total number of time step  $N$  is of course the same for both methods, the multigrid approach takes less execution time. This is probably due to a poor implementation of the defect correction method.

### 5.2 Miscible displacement

The miscible flow problem poses a harder test problem. We consider the case with an adverse mobility ratio  $M = 40$ . For the physical problem to be well-posed we include a velocity dependent dispersion term in our calculation such that the Peclet numbers are given by  $Pe_l = L/D_l = 80$  and  $Pe_t = L/D_t = 800$ . For the characteristic length we take the side of the square that we are simulating. For the interpretation of the numerical results the *mesh* Peclet number is in fact more relevant. The mesh Peclet numbers are defined by  $Pe_{l,h} = \Delta x/D_l$  and  $Pe_{t,h} = \Delta x/D_t$ , where  $\Delta x$  denotes the mesh width. Figure 5.2 shows contour plots of the



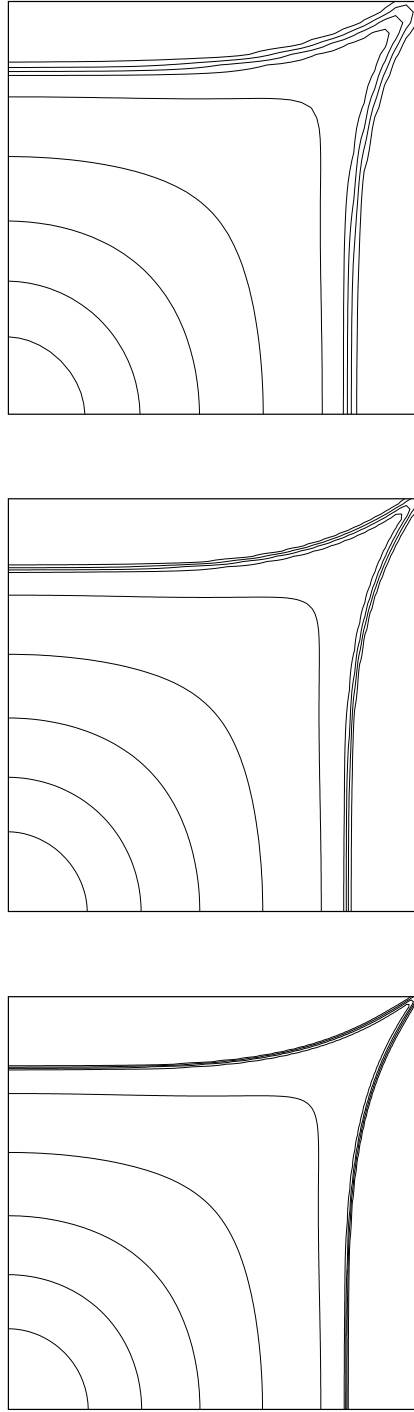


Figure 5.1: Contour plot of numerical solution for immiscible flow problem after 0.45 PVI on the  $40 \times 40$  (top),  $80 \times 80$  (middle) and  $160 \times 160$  (bottom) grid.

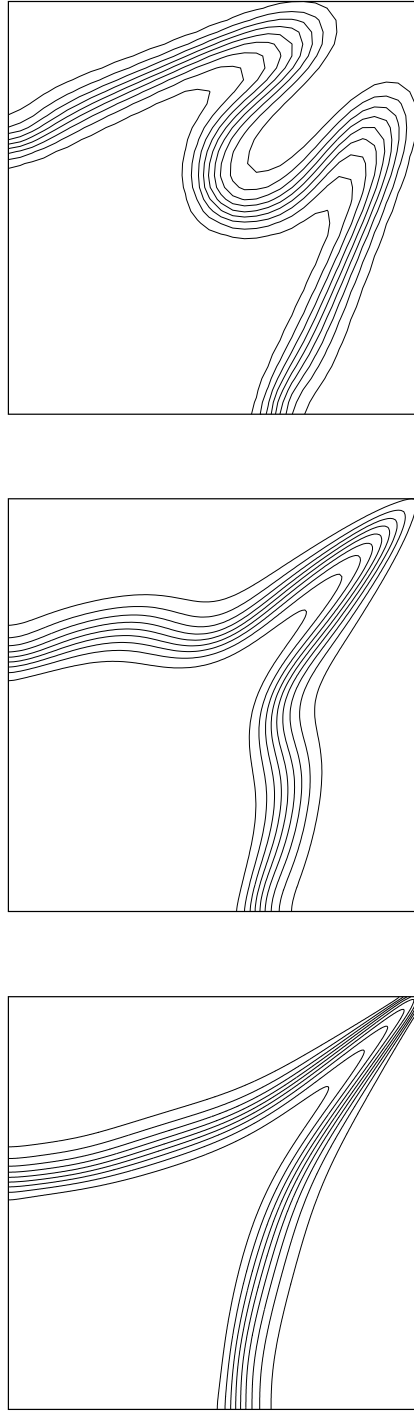


Figure 5.2: Contour plot of numerical solution for miscible flow problem after 0.45 PVI on the  $40 \times 40$  (top),  $160 \times 160$  (middle) and  $640 \times 640$  (bottom) grid.

Table 5.2: Statistics for simulation of miscible flooding.

Grid	$N$	MLTG		DEFCOR	
		$\rho$	$T$	$\rho$	$T$
$20 \times 20$	130	0.09	68	0.03	61
$40 \times 40$	179	0.08	390	0.02	508
$80 \times 80$	195	0.05	1677	0.02	2416
$160 \times 160$	222	0.04	7860	0.02	11774
$320 \times 320$	261	0.04	35291	0.02	53948

$\rho$  average convergence rate,  $T$  total run time

numerical solution on three different grids, whose mesh widths differ mutually by a factor of four. Again these are the results after 0.45 Pore Volume Injected. The numerical solution on the  $40 \times 40$  grid clearly shows grid orientation effects. Two numerical fingers have developed that initially grew parallel to the grid lines. For this calculation the mesh Peclet number is  $Pe_{l,h} = 2$ . Next we consider the solution on the  $160 \times 160$  grid, so with a mesh Peclet number  $Pe_{l,h} = 0.5$ . Now there is a single finger pointing towards the producing well. On the finest grid used, a  $640 \times 640$  grid with a mesh Peclet number  $Pe_{l,h} = 0.125$ , we observe a single, sharp finger growing toward the producing well. These calculations show that finite difference methods can be used for problems in which we expect strong grid orientation effects, provided that the mesh Peclet number is sufficiently small. Table 5.2 shows some simulation statistics. As in the immiscible case, both the multigrid method and the defect correction method exhibits a fast, grid independent convergence behavior. Also for this problem the defect correction approach outperforms the direct multigrid method in terms of the average convergence rate  $\rho$ .

## 6. DISCUSSION

We have considered the use of multigrid methods for high-order accurate fully implicit simulations. Both direct multigrid and the defect correction method perform very well for test problems in which there is a strong coupling between the pressure field and the flow field. The efficiency of both methods, and the moderate memory requirements, allow very fine grid calculations on a standard workstation. The defect correction approach yields a superior convergence behavior for both test problems considered. In terms of total execution time the direct multigrid method is the method of choice. However, this is probably due to a poor implementation of the defect correction approach.

The defect correction approach has the advantage that only first-order accurate discretized problems, with a smaller discretization stencil, have to be solved. Therefore linear multigrid methods that have been developed for first-order accurate discretizations can be used in order to obtain high-order accurate results. In linear multigrid methods it is of course necessary to compute and store the full Jacobean matrix. However for more complicated problems than the ones discussed here, it is anticipated that the disadvantage of the larger memory requirements is easily overcome by the gain in execution speed due to the fact that the different nonlinear functions, and their derivatives, have to be calculated much less often (see

[7]).

Therefore we conclude that the optimal way of applying multigrid for implicit high-order accurate simulations is to use a defect correction method with a linear multigrid solver for the first-order discretized problems.

## REFERENCES

1. J.B. Bell and G.R. Shubin, 'An analysis of grid orientation effects in numerical simulation of miscible displacement', *Comput. Meth. Applied Mech. Eng.*, **47**, 47–71, (1984).
2. A. Bourgeat and J. Koebbe, 'Minimization of grid orientation effects in simulation of oil recovery processes through use of an unsplit higher order scheme', Technical Report 139, iEquipe d'analyse numerique Lyon Sait-Etienne, (September 1992). To appear in "Numerical Methods for PDE".
3. F. Brakhagen and T.W. Fogwell, 'Multigrid for the fully implicit formulation of the equations for multiphase flow in porous media', in *Multigrid Methods: Special Topics and Applications II*, 31–42, GMD, (1990). GMD-Studien 189.
4. J.-A. Désidéri and P.W. Hemker, 'Convergence analysis of the defect-correction iteration for hyperbolic problems', *SIAM J. Sci. Statist. Comput.*, **16**, 88–118, (1995).
5. *The mathematics of reservoir simulation*, ed., R.E. Ewing, Frontiers in applied mathematics, SIAM Publications, 1983.
6. B. van Leer, 'Towards the ultimate conservative difference scheme V. A second order sequel to Godunov's method', *J. Comput. Phys.*, **32**, 101–136, (1979).
7. J. Molenaar, 'Multigrid methods for fully implicit oil reservoir simulation', Technical Report 95-40, T.U. Delft, (1995). To appear in "Proceedings Copper Mountain Conference on Multigrid Methods 1995".
8. M.R. Todd, P.M. O'Dell, and G.J. Hirasaki, 'Methods for increased accuracy in numerical reservoir simulators', *Soc. Pet. Eng. J.*, **12**, 515–530, (1972).